

STUDY OF EXPERIMENTAL TECHNIQUES FOR FATIGUE STRESS MEASUREMENT IN OVERHEAD CABLES FOR POWER LINES

Thamise Sampaio Vasconcelos Vilela

Universidade de Brasília – UnB, Campus Universitário Darcy Ribeiro, Brasília-DF, cep: 70910-900
 thamisevilela@yahoo.com.br

Aida Alves Fadel

Universidade de Brasília – UnB, Campus Universitário Darcy Ribeiro, Brasília-DF, CEP: 70910-900
 aida@umb.br

Jorge Luiz de Almeida Ferreira

Universidade de Brasília – UnB, Campus Universitário Darcy Ribeiro, Brasília-DF, CEP: 70910-900
 jorge@umb.br

José Alexander Araújo

Universidade de Brasília – UnB, Campus Universitário Darcy Ribeiro, Brasília-DF, CEP: 70910-900
 alex07@umb.br

Abstract. Mechanical failure in overhead conductors of power lines results from fretting fatigue provoked by vibration, what is generated by wind flow acting over the surface of the conductor. the failure happens usually on the last point of contact (LPC) of cable/suspension clamp assembly, used to fix the conductor to the towers. the present experimental work aims to reassess and evaluate techniques for mechanical stress, σ_a , determination, which is obtained through: i) the use of bending amplitude at a point 89 mm apart from the lpc (direct measurement, Y_B), what will then be applied to Poffenberger-Swart formula (P-S), or, ii) the maximum amplitude of deformation, ϵ_a , due to bending deflection Y_B , measured with a strain gage at lpc, to be used at hooke's law. p-s expression faces the cable/clamp interface as an euler beam, in order to correlate the peak-peak displacement caused by vibration of the conductor, Y_B , the a nominal stress level (at the failure region), but although some important parameters to define the problem, such as contact forces, are not described by this expression, it has been used almost exclusively to determine cable's life expectancy. dynamic tests are carried out in a frequency range of 15-25 Hz, close to a chosen resonance peak and keeping the amplitude, which will be chosen range between 0.2 and 1.0 mm, while the tested sample is stretched with a load that is 20% of it is RTS. results shows that experimental values exhibit a good agreement with the nominal stress calculated by using the P-S formula.

Keywords: overhead conductors, fretting fatigue, Poffenberger-Swart, strain gages.

1. INTRODUCTION

The conductor is the most important element in a transmission line, since is the structure responsible for carry out the electricity. It enhances predictive and preventive maintenance play in order to avoid unexpected failures, resulting in no electricity supply, and it's consequences to economy, among others.

Most failures in power cables involve material fatigue, resulting by Aeolian vibration, caused by the action of wind flow acting transversally to the conductor. As any fatigue mechanical problem the amplitude of the movement (the severity of vibration), and it's frequency will define life expectancy of the transmission line.

Normally, conductor failure is observed at the movement restraining points, such as suspension clamps, dampers, etc., (Rawlins, 1979, Cigrè, 1985, Cigrè, 2006), being more frequently observed at suspension clamps (Figure 1).



Figure 1 – Typical fatigue failure in overhead conductors, (Cigrè, 2006).

Thamise Vilela, Aida Fadel, Jorge Luiz Ferreira and José Alexander Araújo

Study of Experimental Techniques for Stress Fatigue Measurement in Overhead Cables for Power Lines

Having the wind as excitation source, the aerial conductors are subject to three types of movements: Aeolic vibration, sub-span vibration (bundles) and conductor galloping (Rawlins, 1979, EPRI, 1979). The first, results from conductor standing alone, at the airflow, where vortex-shedding-induced vertical vibrations – characterized by low amplitudes and high frequencies –, are observed. The second type occurs in bundle assemblies, when the vortex coming from the front conductor in the bundle induces vibrations in both vertical and horizontal planes of the cable aside. However, there is another form of action of the wind over the conductor, known as galloping, more common at colder climates, where the accumulation of ice on the conductor modifies its aerodynamic stability by generating an unbalanced load problem, in this case vibration is characterized by low frequencies and high amplitudes. Although this third case may occur in Brazil, it is quite improbable, unless when the unbalance mass is something like a warning sphere, used for preventing airplanes shock to the lines, for instance (Fuchs, et al, 1992).

Certainly Aeolic vibration is the most recurrent and more dangerous of the vibration types, therefore, usually inspires greater care when designing and establishing maintenance routines for transmission line.

The conductor fits the suspension clamp curvature all along the clamp (Figure 2). According to the severity of vibration, the dynamic amplitude imposed near the restriction point, may result that, the wires forming the conductor layers will have more or less contact/slippery to each other and to the clamp. It was noticed that fatigue failures in these structures are strongly influenced by the local contact problem (Cigrè, 2008).

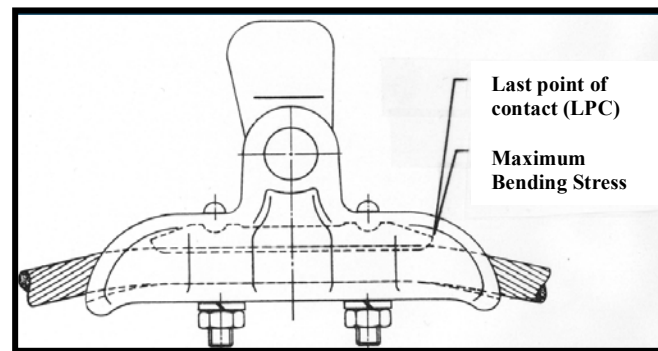


Figure 2 – Suspension clamp/cable assembly schematic, (Cigrè, 2008).

The characteristic failures occur at the contact points where the cracks start to grow, as can be seen at Figure 3A. Hence the problem refers to fretting fatigue phenomena (Zou, *et al*, 1994, Cloutier, *et al.*, 2006). These cracks, caused by combined process of abrasion (fretting) and cyclic loading of the cable invariably occur on the surfaces of contact between the suspension clamp and cable, or contact between the wires [Ramey, *et al.*, 1981, Cardou, A., *et al.*, 1994, Azevedo, C.R., *et al*, 2009], as can be seen at Figure 3B. Hills and Nowell, 1994 showed that the fatigue strength of metals under conditions of fretting was substantially reduced with respect to fatigue without fretting (Zhou, *et al*, 1992, Zhou, *et al*, 1997).

Fretting fatigue is a mechanical and metallurgical phenomenon that occurs when components, clamped under variable loading, suffer relative tangential motions. In the contact areas, wear and corrosion are observed, these rates will vary depending on three conditions: *i*) contact characteristics (normal load, amplitude of slip, frequency), *ii*) surface characteristics (composition, surface roughness, residual surface stresses, presence of surface films, etc.) and, *iii*) environmental characteristics (temperature, oxidizing atmosphere, presence of water vapor, etc.), (Waterhouse, 1992).

The process of fretting fatigue follows three main stages: *i*) crack initiation, *2*) debris generation, and *3*) steady-state stage (Hurricks, 1970). First of all, slipping or sliding, erodes the thin layer of oxides existing at the surface of the bodies in contact. The bare surfaces come in direct contact forming microwelds, what results in an increase of the friction coefficient (Endo and Goto, 1976). At this point, the fine powder generated by the continuous wear combined with the atmosphere oxygen, turns into oxides, forming a third body (a fine “cocoa” in the case of steel, a dark powder in the case of aluminium). These materials are usually much more hard than the base material (Azevedo *et al*, 2009). Then, we begin to observe the plastic deformation of the faces and the formation of more debris (Figure 3C). Microcracks start to appear. It is mainly the amplitude of sliding or slipping, and the axial loading used to stretch the conductor, that determines the rate of propagation of these cracks, if they will be ground away or if they will join in order to promote the formation of larger debris (Araújo, *et al.*, 2008).

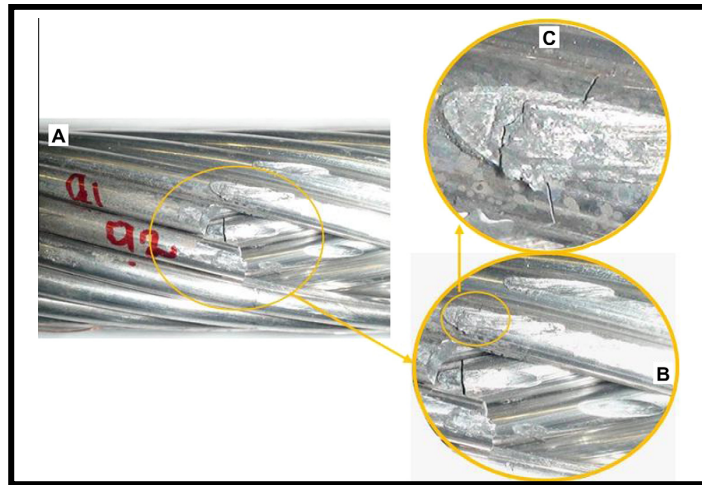


Figure 3 – (A) Strand failures at fretted areas in the, (B) internal and (C) external layer (zoomed view), (Fadel et al., 2011).

Compared to classical fatigue cases, the initiation of cracks is obviously quicker when there is fretting. Hence, the life of parts under fretting is drastically reduced. However there is a reverse behavior as slip amplitude increases, the increased wear rate tends to wear out cracks before they are able to propagate. Based on these facts, it appears that the fretting behavior of the conductor will strongly depend on the amplitude of vibration (which influences the slip and wear inside the contact areas), the clamping systems (which induces their own fretting behavior), and lubrication of the interface (lubrication reduces oxidation, increases slippery and diminishes the tangential forces) (CIGRE, 2007). The importance of contact stresses is thus obvious. In order to analyze them, it is of interest to know the actual stretching loading on the conductor during a fatigue test (Fadel, *et al.* 2010).

With this in mind, we applied strain gauges at wires near the critical contact points to check the validity of the nominal stress calculated by P-S formula (Poffenberger and Swart, 1965), and proposed as representative of the failure inducing stress, since the real point of failure, often happens to be inside the clamp.

According to the Poffenberger-Swart model, the vertical displacement (measured peak to peak) of a point 89 mm apart from the last point of contact between the cable and suspension clamp, (LPC), is associated with the nominal stress in an aluminum wire in the outermost layer of the cable and positioned into the mouth of the clamp. Another way to obtain this stress is by measuring voltage experienced by a strain gage as can be seen at Figure 4. To determine dynamic bending strain, ϵ_a , which will lead to the stress by applying Hooke's Law and finally compare the experimental bending stress to the value calculated by P-S formula.

Cardou *et al.*, 1994 and Zhou *et al.*, 1996 pointed out a limitation in the formula for the fracture of the wire is caused not only by the alternated motion of the cable, but also by a state of tension arising from an extremely complex mechanical contact under the regime of partial slip. Despite these restrictions the P-S formula has been an important tool for assessing the severity of vibration levels in power cables, for over thirty years, due to its direct and simple way of converting bending amplitude into idealized stress amplitude. This work consists in present the methodology being followed and the experimental data obtained from conductors tested which will be then compared to the alternating P-S (Poffenberger-Swart) stress, σ_a , what is used to build S-N curves, generating a tool to access fatigue endurance.

2. NOMINAL STRESS AMPLITUDE CALCULATED BY P-S (Poffenberger-Swart, 1965)

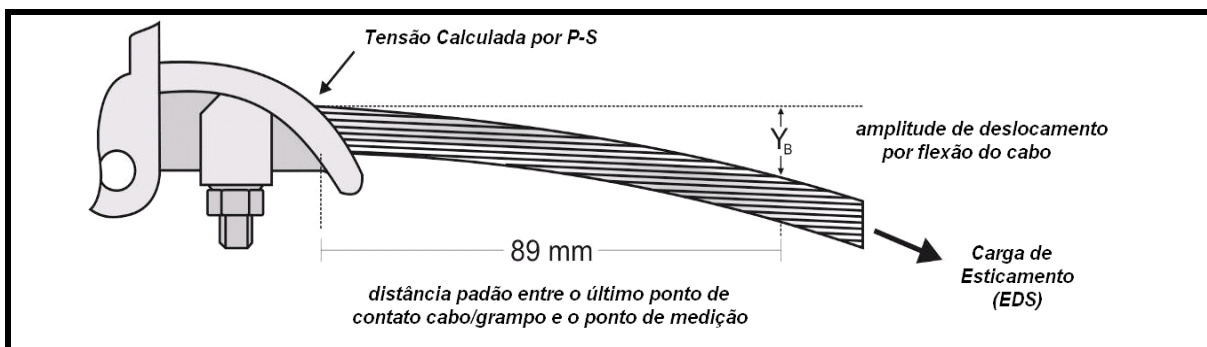


Figure 4 – Position of strains at LPC.

Thamise Vilela, Aida Fadel, Jorge Luiz Ferreira and José Alexander Araújo

Study of Experimental Techniques for Stress Fatigue Measurement in Overhead Cables for Power Lines

As expressed by the Equation 1, Poffenberger–Swart (P–S) expression is based on Bernoulli–Euler beam theory and assumes that the conductor works as a fixed cantilever beam under axial loading, with a prescribed vertical displacement at the free edge, as shown at Figure 5 have been widely used (Poffenberger and Swart, 1965). It relates bending amplitudes, measured at a reference distance from the fixing, to stresses in an aluminium wire of the conductor outer layer. (Figure 4). More specifically it can be written as:

$$\sigma_a = kY_B \text{ [MPa]} \quad (1)$$

Where, σ_a is the dynamic bending stress amplitude (zero to peak), Y_B is the conductor's vertical displacement range (peak to peak), measured at 89 mm from the last point of contact (LPC) between cable and clamp, and the Poffenberger parameter, K , is given by

$$k = \frac{E_a d p^2}{4(e^{-px} - 1 + px)} \text{ [N/mm}^3\text{]} \quad (2)$$

Where,

E_a (MPa) and d (mm) the Young's modulus and the diameter of an aluminum wire in the outer layer, respectively;
 x is the distance on the cable between the last point of contact between cable and clamp and the vertical displacement measuring point (usually $x = 89$ mm) (Figure 4).

$$p = \sqrt{\frac{T}{EI}} \quad (3)$$

Where, T (N) is the static conductor tension (everyday stress, EDS) at average ambient temperature during test period and, EI (N.mm²) is the flexural stiffness of the cable, whose minimum value is:

$$EI_{min} = n_a E_a \frac{\pi d_a^4}{64} + n_s E_s \frac{\pi d_s^4}{64} \quad (4)$$

Where, n_a , E_a , d_a are the number, individual diameter and Young's modulus of the aluminium wires and n_s , E_s , d_s are the respective values for the steel wires. In this approach, the conductor is considered as a bundle of individual wires free to move relatively to each other and flexural stiffness take its minimum value EI_{min} . For smaller bending amplitudes, the individual strands would stick together thus the conductor would behave as a solid rod, increasing the flexural stiffness to its maximum. The formula that consider the stick–slip theory to compute EI and hence the dynamic bending stress were proposed elsewhere (Papailiou, 1995 and 1997) but will not be addressed in this work.

3. TEST PROCEDURE, MATERIALS AND NOMINAL STRESS

3.1 Fretting fatigue rig for conductors fatigue test

A fretting fatigue rig composed by two benches was designed to carry out tests on overhead conductors. This test apparatus is an enhanced version of a single bench, previously mounted the University of Brasília and described by the authors elsewhere (Henriques, 2006, Azevedo *et al.*, 2009 and Fadel, 2010), therefore just a brief description will be provided here. Figure 5 depicts a schematic view of such rig. The fatigue bench is approximately 47 m long. It is divided in two spans: active (42 m) and passive (5 m). The cable is anchored in a fixed block (at the passive span). It is assembled in a monoarticulated suspension clamp attached to a metallic cradle, which lays over a moveable concrete block that can be displaced over a 12 m rail track. An electronically controlled shaker is used to simulate the Aeolian vibration. The shaker is connected to the cable within the active span. At the right edge of the active span the cable is connected to a lever arm loaded by a dead weight, which stresses the cable.

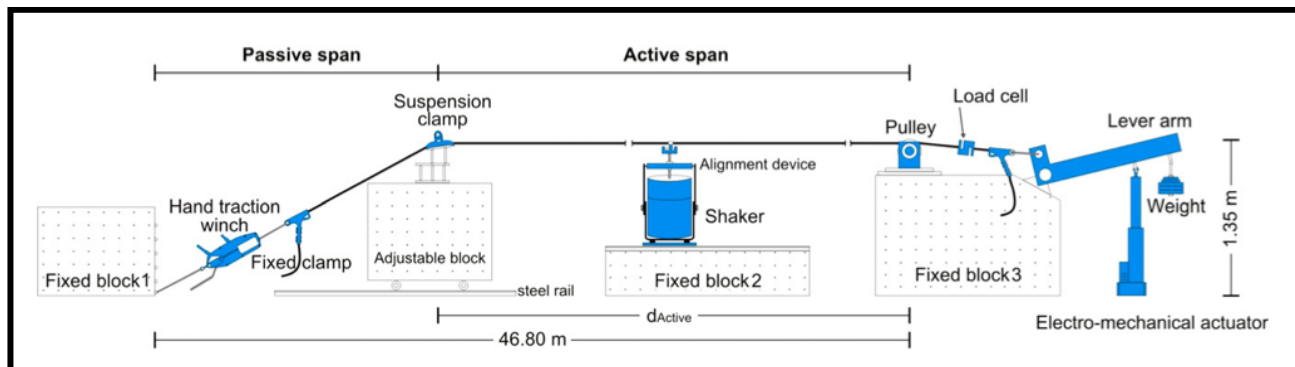


Figure 5 - Schematic view of the fretting fatigue rig for overhead conductors

Apparatus adjustments will be described here, in more detail, as the information can be useful for other researchers interested in carrying out this type of experiment. Usually electronically controlled shakers are extremely sensitive to misalignments and side loads. Although extreme care was taken to position the shaker on its trail and connect it to the cable in order to minimize misalignments, temperature variations and creep could still provoke small changes in cable length.

To provide further protection to the system and to increase the quality and repeatability of the tests, the laboratory environment was conditioned (tests are performed at $20 \pm 1^\circ\text{C}$) and an isolator transformer installed to provide electrical stability.

3.2 Materials and test procedures

3.2.1 Materials

Tests were carried out on two cables: Ibis - 397.5 MCM and T-Grosbeak - 636 MCM, which are used in transmission lines. Test samples were provided by Nexans. These two conductors are known as ACSR (Aluminum Conductor Steel Reinforced) or CAA (cables bare aluminum Steel Reinforced), which are concentrically stranded with one or more layers of aluminum wire 1350-H19, for Ibis, or aluminum-alloy thermo-resistant to T-grosbeak on the steel core (Figure 6).

The cables meet the specifications in Brazil ABNT NBR7270/88 according to the supplier (Nexans, 2007). Both conductors have 7 strands at their core, 10 at the internal layer and 16 at the external layer. The difference is at the diameter of the wires and the external nominal diameter, as can be seen at Table 1.

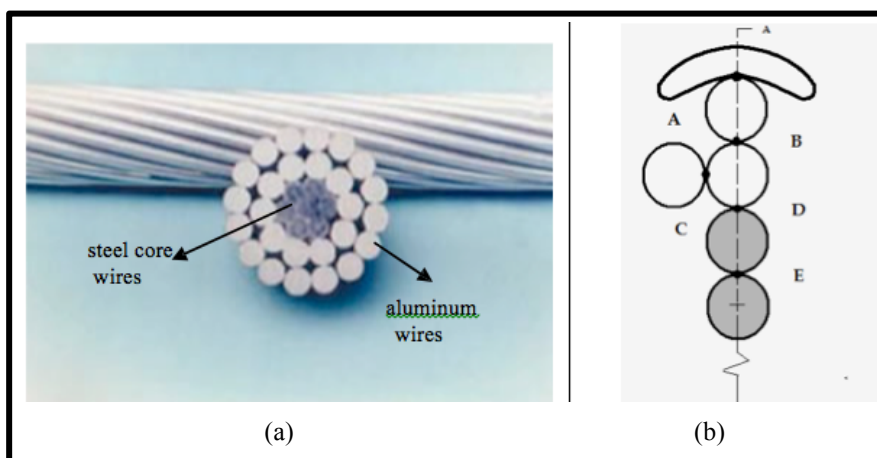


Figure 6 – (a) Photo of an ACSR conductor, (b) Contact regions, (Fadel, 2010).

Thamise Vilela, Aida Fadel, Jorge Luiz Ferreira and José Alexander Araújo

Study of Experimental Techniques for Stress Fatigue Measurement in Overhead Cables for Power Lines

Table 1 and Table 2 shows number of wires, dimensional and structural characteristics of the conductors and the mechanical properties of the aluminum.

Table 1 - Dimensional and structural characteristics of the conductor (NEXANS, 2007)

CONDUCTOR	CONDUCTOR CROSS SECTION MCM	CROSS SECTION [MM ²]			(# WIRES X DIAMETER)		NOMINAL DIAMETER [MM]	LINEAR WEIGHT [KG/KM]	RUPTURE LOAD [KGF]
		ALUMINIUM	STEEL	TOTAL	ALUMINIUM	STEEL			
Ibis	397,5	201,21	32,79	234	26x3,139	7x2,441	19,88	557,5	7394
T-Grosbeak	636	322,33	52,47	374,8	26x3,973	7x3,089	25,16	1302,8	11427

Table 2 –350-H19 aluminum properties. (Fadel, 2010).

MECHANICAL AND PHYSICAL PROPERTIES	UNIT	VALUE
Poisson Coefficient	-	0,33
Density	Kg/m ³	2705
Brinell Hardness	-	50
Elongation (Min)	%	1,5
Yield Strength	MPa	165
Tensile Strength	MPa	186
Modulus of Elasticity	GPa	68,9
Fatigue Strength to 5x10 ⁸ Cycles	MPa	48,3
Shear Strength	MPa	103

The suspension clamps are made of a high strength (corrosion resistant), non-magnetic cast aluminium alloy with 68.6 kN rated tensile strength (RTS). The suspension clamp is smooth and uniform, have no sharp edges and its “mouth” has a maximum output angle of 20° in order to prevent damage to the cables (Figure 7).

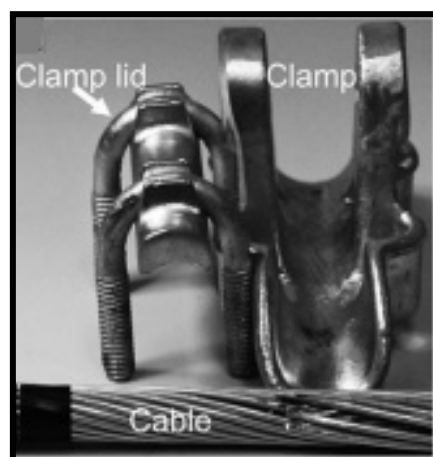


Figure 7 - Cable sample and suspension clamp components.

For tests conduction were used electrical resistance strain gages (ERS) that are suitable for aluminum, unidirectional simple and traditional way. The bridge gage used was set to ¼ bridge in logger ADS2000, in an arrangement with two wires and a compensating internal 350 Ω and 7.5 VDC supply stabilized.

3.2.2 Test procedure

The control parameters for these tests are the frequency and the bending amplitude, peak-peak, at the point 89 mm, according to IEEE standard (Poffenberger and Swart, 1965, Papailiou, 1995).

Tests were conducted according to the following previous procedure:

1. Once the conductor sample is positioned at the test rig, both extremities are tied to the fixed blocks 1 and 3 (see Figure 5);
2. Application of static loading, using the hand traction winch and weights suspended by the lever arm, from 0 to 20% RTS;
3. The conductor is put to rest over the night;
4. Cable sample is then adjusted over the cradle of the clamp, over the mobile block, where a set of wedges is adjusted beneath the plate where the suspension clamp lies on, aiming to simulate the sag angle between cable and clamp in-field (here taken as 10°), as can be seen at Figure 9b;
5. Upper part of the clamp is the positioned and locking system is the activated by tightening the pair of U-bolts bolts with a 50 N.m torque applied to the nuts that fix the assembly;

Sample is then instrumented with three strain gauges at the wires of the outermost layer of the conductor at the LPC, as shown at Figure 8 below: one wire at the top (center) of the cable and the other two on the adjacent wires. The gages were then labeled left, center, and right based on their location. Subscripts L, C, and R will henceforth be used.

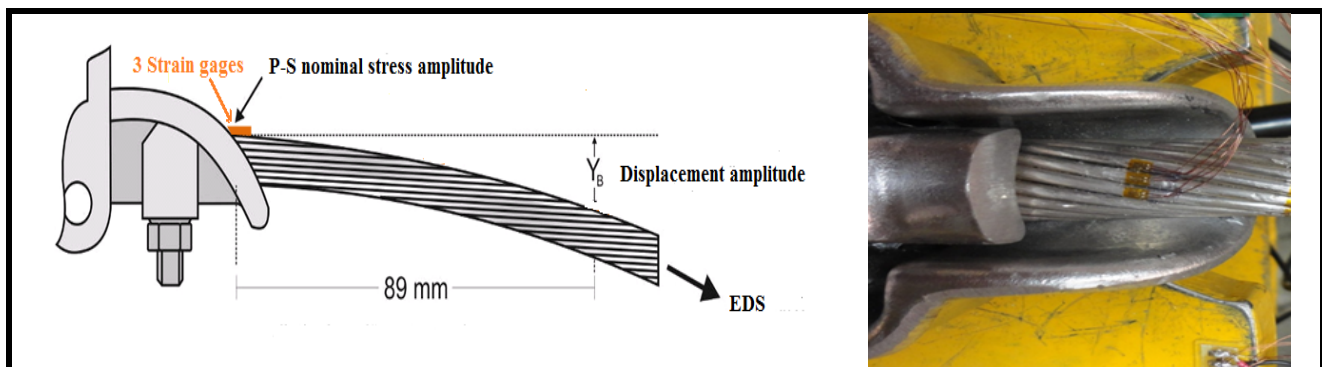


Figure 8 – Positioning of strain gauges (ERS) in relation to the mouth of the clamp (adapted from Fadel, 2010).

These strain gauges have its working principle based on the resistance change that occurs in a wire when its cross section is changed and provide a direct reading of strain (ϵ) suffered at the point of the wire instrumented conductor which correlates with the amplitude of stress (σ), by Hooke's law (Eq. 5):

$$\sigma = E \epsilon \quad (5)$$

Where E is the modulus of elasticity (Young's modulus) of aluminum wire, in which the strain gauge is glued.

To perform the tests two PCB accelerometers are placed: one at the connection between shaker and cable (see Figure 9a), will measure Y_{shaker} and another at the point 89 mm, will measure Y_B (see Figure 9b).

First step is to identify the natural frequencies of the sample in the test, what is obtained by placing the control at Y_{shaker} and measuring the response at the point 89 mm and the carrying out sweep in frequency under some prescribed range (here between 15 and 25 Hz), and extracting the rate between Y_B (Y_{89mm}) and Y_{shaker} .

Once the natural frequencies are identified one of them must be chosen considering the limitations of the equipment related to the power it can provide.

Control is the placed at the Y_B (Y_{89mm}) point, to carry out the stress measurements. Y_B value is kept under prescribed value, with uncertainty smaller than 0.01 mm, as the test is controlled by closed loop where a PCB accelerometer at the point 89 mm (output) feeds the shaker behavior (Y_{shaker}).

Despite the high number of conductor's natural frequencies (Kiessling et al., 2003) verified by the sweep procedure (an average of 2,0 Hz between the resonant frequencies), just some vibrations modes will guarantee that the power limit of the shaker will not be reached and that only vertical vibration will occur in the active span, as desired. The appropriate mode frequency is then chosen as high as possible to reduce test duration. Typical frequencies are chosen between 18 and 25 Hz.

Thamise Vilela, Aida Fadel, Jorge Luiz Ferreira and José Alexander Araújo

Study of Experimental Techniques for Stress Fatigue Measurement in Overhead Cables for Power Lines

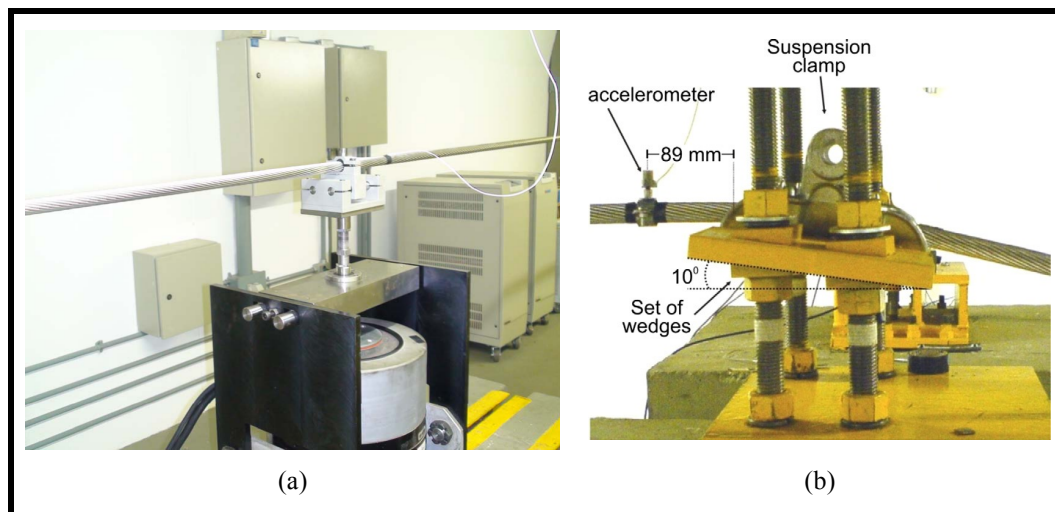


Figure 9 - Location of PCB accelerometer (a) cable/shaker connection (b) point 89mm, Fadel, 2010.

To collect the experimental data register from the strain gauge (ϵ_a), the chosen bending amplitudes adopted for all conductors are 0.2, 0.4, 0.6, 0.8, 1.0 and 1.2 mm and data were collected during 2 minutes for each test to an acquisition frequency of 500 Hz.

4. RESULTS

Tests were conducted within a range of 15 to 25 Hz (according to better stability shown while conducting the test) under an EDS of 20% (traction load of 20% of the RTS) what corresponds to 1480 kgf for Ibis and to 2250 kgf for Grosbeak.

Strain gages had similar arrangement in both conductors: Ibis and Grosbeak (Figure 8).

For each given, dynamic amplitude of displacement, Y_B , peak-peak imposed at the point 89 mm, P-S formula (Eq. 1) provided a calculated value for the bending stress amplitude (0-peak) at LPC.

Here it is important to emphasize that, although all tests were conducted under displacement control, as detailed at the end of Section 3.2.2, it is possible to run different tests imposing different Y_B , in order to obtain the same nominal stress, when it will be of some interest.

Therefore, for sake of comparison, Table 3 and Table 4 present for each given Y_B (column 1) the values of nominal stress obtained through the application of Hooke's Law (Eq. 5), to the strain provided by each strain gauge according to its position taken as reference the active span as shown at Figure 8: right position at column 2, center position at column 2 and left position at column 3. Column 4 presents the average value of the previous three ones, representing the average experimental stress. Column 5 shows the nominal stress calculated by P-S, considering the data provided by Tables 1 and 2 and the Equations from 1 to 4.

Figures 10 and 11 presents a graphic comparison between experimental and theoretical stress values for each imposed dynamic displacement, Y_B , according to Tables 3 and 4, respectively.

Table 3 - Strain gage test results under dynamic loading condition to Ibis conductor.

Ibis					
Yb [mm]	Tensão [Mpa]				
	R	C	L	Media	P-S
0,2	7,09	7,46	7,25	7,27	7,24
0,4	13,35	13,81	13,54	13,57	14,48
0,6	18,33	19,67	21,82	19,94	21,73
0,8	25,14	26,76	28,27	26,72	28,97
1,0	29,95	31,08	33,28	31,43	36,21
1,2	37,09	36,11	38,96	37,38	43,45

Table 4 - Strain gage test results under dynamic loading condition to T-Grosbeak conductor.

Grosbeak					
Yb [mm]	Nominal Stress [Mpa]				
	R	C	L	Media	P-S
0,2	6,94	9,65	7,04	7,88	6,85
0,4	12,56	17,53	12,99	14,36	13,70
0,6	17,68	24,76	18,26	20,23	20,55
0,8	23,63	30,37	24,14	26,05	27,40
1,0	26,75	33,62	30,06	30,14	34,25
1,2	34,66	30,05	41,92	35,54	41,10

At the graphic shown at Figure 10, the equation $\sigma_{P-S} = 36,2508 Y_B$, was obtained through the linear fitting of P-S data presented at Table 3. Analogously the equation $\sigma_{Exp} = 32,009 Y_B$ was obtained by the linear fitting of the average experimental data (column 5 of Table 4), which is shown at the graphics as a square dot. Fitting of both curves show a good agreement between P-S estimative and the measured value, what can be corroborated by the fitting parameters: $R^2=1$ and $R^2=0,9929$.

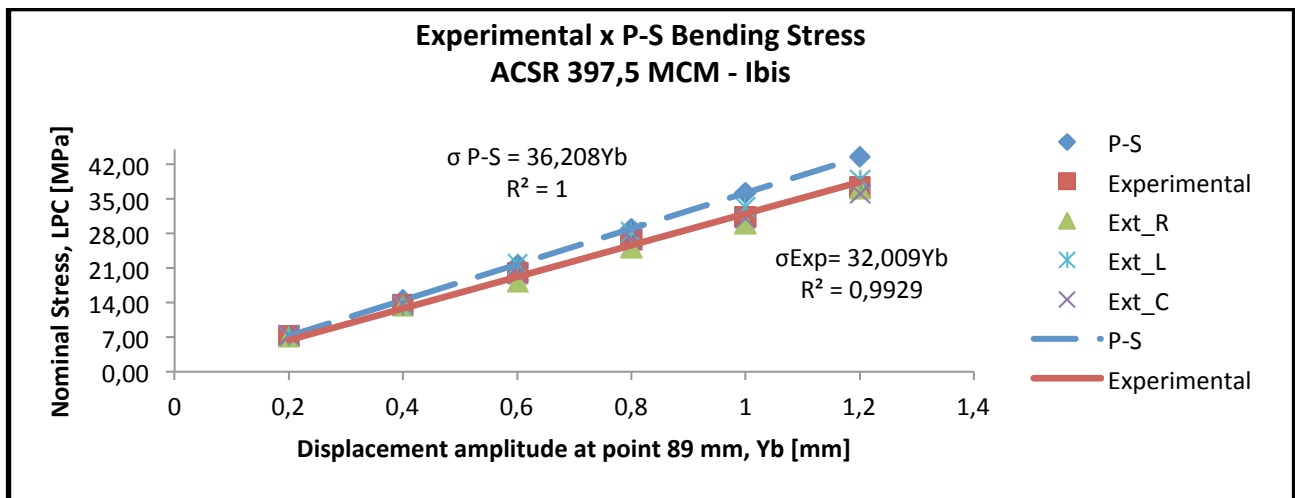


Figure 10 – Comparison among theoretical (P-S) and experimental bending stress data for an Ibis conductor.

Figure 11 depicts the behavior of both experimental and theoretical data, and analogously, to the previous graphic the equation $\sigma_{P-S} = 34,252 Y_B$, was obtained through the linear fitting of P-S data, and the equation $\sigma_{Exp} = 31,07 Y_B$ was obtained by the linear fitting of the average experimental data (column 5 of Table 3), which is shown at the graphics as a square dot. Fitting of both curves show a good agreement between P-S estimative and the measured value, what can be corroborated by the fitting parameters: $R^2=1$ and $R^2=0,9929$.

In both graphics (Figures 10 and 11) it is possible to observe that the fitting start to lose quality as Y_B grows.

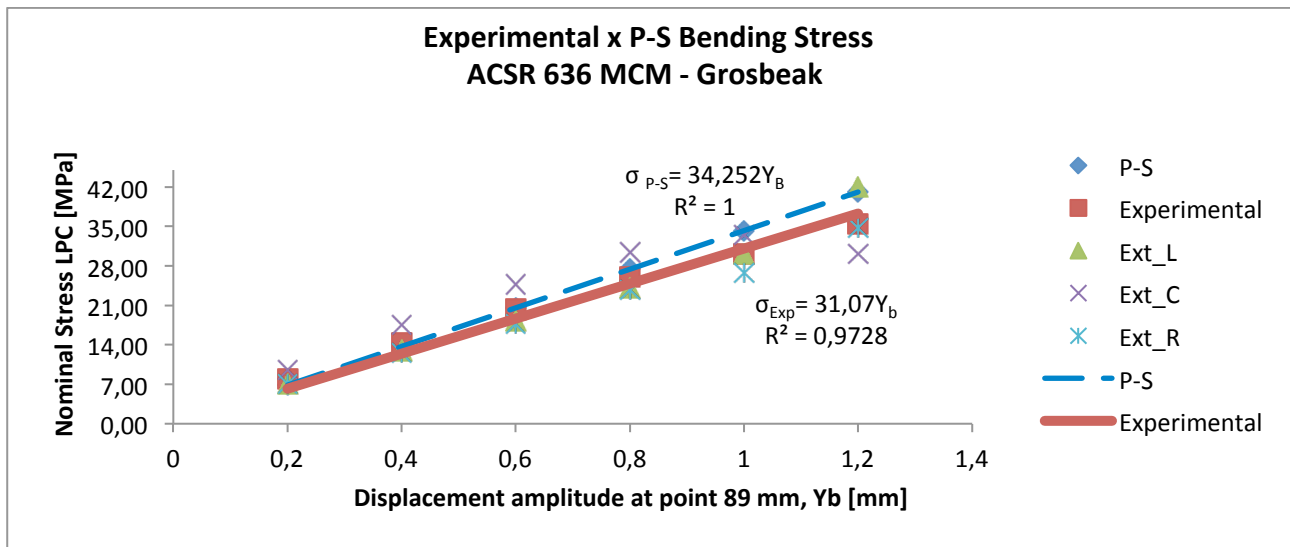


Figure 11 - Comparison among theoretical (P-S) and experimental bending stress data for a Grosbeak conductor.

5. DISCUSSION

This work was essentially of experimental nature. The main purpose was to evaluate the Poffenberger–Swart formula, which provides alternating bending stresses, σ_a , that are usually used as fatigue endurance indicator for overhead conductors design and maintenance.

These alternating stresses are used to regroup the fatigue results from the different conductors. P-S correlated well with fatigue data. It is assumed that each strand of the taut conductor bends independently (minimum bending stiffness hypothesis) and that the boundary conditions at the ends of the conductor correspond to a fixed square-faced bushing. The equation gives different results since they are obtained by using different amplitude parameters (Y_B). Stresses were computed from the alternating strains obtained from the gauges located at the closest axial positions to the LPC.

In the case of overhead conductors the fatigue inducing stresses at the contact between individual wires or between the external wires and the clamp surface are not accessible to direct measurement neither by estimation of any sort (analytical or numerical procedure) due it is not an easy task because of the complexities involved in inner conductor mechanics (plasticity, variable flexural stiffness and wear resulting from partial slip contact regime, etc.) (Papailiou, 1997).

Both conductors tested were ACSR type with conventional geometry, and for both experimental results were very good, when compared to P-S. The slightly worse results at higher bending displacements could be explained by an increase of the bending stiffness, once Equation 4, considers the superposition of an independent contribution of every wire to compute stiffness, what tends to be far from true as bending amplitude increases and contact among wires becomes more strong, once the conductor behaves more as a solid shaft.

6. CONCLUSION

When the conductor is dynamically loaded, the values measured by strain gauges placed at the last point of contact stress curves as a function of displacement amplitude, Y_B , imposed at the point 89 mm, shows good agreement with the calculated curve by P-S formula. Therefore, P-S proves to be a reasonable fatigue project parameter. However, it is necessary a fatigue indicator that would better fit the physics of the problem, once the inner contact works as an accelerator of the conductor damage. The effect of variables, such as the clamping pressure, on cable's fatigue durability can be implicitly detected by the nominal stress computed according to the P-S (Poffenberger and Swart, 1965) just if tests are carried out.

7. REFERENCES

- Araújo, J.A., Susmel, L., Taylor, D., Ferro, J.C.T. and Ferreira, J.L.A., 2008. On the prediction of high cycle fretting fatigue strength, theory of critical distances vs. hot spot approach. *Eng Fract Mech*; 75:1763–78.
- Azevedo, C.R.F., Henriques, A.M.D., Pulino Filho, A.R., Ferreira, J.L.A. and Araújo, J.A., 2009. Fretting fatigue in overhead conductors: rig design and failure analysis of a Grosbeak aluminium cable steel reinforced conductor. *Eng Fail Anal*;16:136-51.

- Cardou, A., Leblond, A., Goudreau, S. and Cloutier, L., 1994. Electrical conductor bending fatigue at suspension clamp: a fretting fatigue problem. *Fretting fatigue*. ESIS 18. London: Mechanical Engineering Publications; p. 257–66.
- CIGRE ,WG 11 SC B2 , 2006. “Fatigue Endurance Capability of Conductor/Clamp Systems Update of Present Knowledge”, Jan.
- CIGRE SCB2 WG11 TF7, 2007. Fatigue endurance capability of conductor/clamp systems-update of present knowledge. TB # 332, Paris.
- CIGRE SCB2-08 WG30 TF7, 2008. Engineering guidelines relating to fatigue endurance capability of conductor/clamp systems.
- CIGRE SC22-WG04, 1985. Guide for endurance tests of conductors inside clamps. *Electra*, No 100; p. 77–86.
- Cloutier, L., Goudreau, S., and Cardou, A., 2006 “Chapter 3: Fatigue of overhead conductors,” in *EPRI Transmission Line Reference Book: Wind-Induced Conductor Motion*. Palo Alto, CA: EPRI.
- De Groot M.H. and Schervish, M.J., 2001. *Probability and statistics*. 3rd ed. Addison-Wesley.
- Endo, K. and Goto, H., 1976. “Initiation and propagation of fretting fatigue cracks,” *Wear*, vol. 38, pp. 311–324.
- EPRI, 1979. *Transmission line reference book: “The Orange Book”*. Palo Alto (CA): Electric Power Research Institute.
- Fadel, A.A., 2010. *Avaliação do Efeito de Tracionamento em Elevados Níveis de EDS Sobre a Resistência em Fadiga do Condutor IBIS (CAA 397,5 MCM)*. Tese de Doutorado. Brasília, DF, Brasil: Universidade de Brasília. 185 p.
- Fadel, A. A. ; Rosa, D. ; Murça, L. B. ; Ferreira, J.L.A. ; Araújo, J. A. . Effect of high mean tensile stress on the fretting fatigue life of an Ibis steel reinforced aluminium conductor. *International Journal of Fatigue*, 2011, doi:10.1016/j.ijfatigue.2011.03.007.
- Fuchs, R. D., Almeida, M. T., Labegalini, P. , 1992. “*Projetos Mecânicos de Linhas Aéreas de Transmissão*”, 1ª. Ed. Itajubá:Edgard Blücher, 252p.
- Henriques, A.M.D., 2006. *Bancada de Ensaios Mecânicos à Fadiga de Cabos Condutores de Energia*. Tese de Doutorado em Estruturas e Construção Civil, Universidade de Brasília – UnB, Faculdade de Tecnologia, Departamento de Engenharia Civil e Ambiental.
- Hills, D.A and Nowell D., 1994. *Mechanics of fretting fatigue*. Dordrecht: Kluwer Academic publishers.
- Hurricks, P. L., 1970. “Mechanism of fretting,” *Wear*, vol. 15, pp. 389–409.
- Kiessling, F., Nefzger, P., Nolasco, J.F. and Kaintzyk, U., 2003. *Overhead power lines: planning, design construction*. Berlin: Springer.
- Lévesque, F., Goudreau S., Cardou, A. and Cloutier, L., 2010. Strain Measurements on ACSR Conductors During Fatigue Tests I – Experimental Method and Data. *IEEE TRANSACTIONS ON POWER DELIVERY*, VOL. 25, NO. 4.
- NEXANS, 2007. *Catálogo do Fabricante – Características dos cabos ACSR/CAA*.
- Poffenberger, J.C. and Swart, R.L., 1965. Differential displacement and dynamic conductor strain. *IEEE Trans*; PAS-84:281–9.
- Papailiou, K.O., 1997. On the bending stiffness of transmission line conductors. *IEEE Trans Power Deliver*;12:1576–88.
- Papailiou, K.O., 1995. Improved calculations of dynamic conductor bending stresses using a variable bending stiffness. *CIGRE, SC 22 WG11*. Madrid; [paper 22-95(WG 11)-138].
- Ramey, G. E. and Townsend, J. S., 1981. “Effect of clamp on fatigue of ACSR conductors,” *J. Energy Div. ASCE*, vol. 107, pp. 103–119.
- Rawlins, C. B., 1979. “Chapter 2: Fatigue of overhead conductors,” in *Transmission Line Reference Book—Wind-Induced Conductor Motion*. Palo Alto, CA: EPRI.
- Waterhouse, R. B., 1992, “Fretting fatigue,” *Int. Mater. Rev.*, vol. 37, no. 2, pp. 77–97.
- Zhou, Z.R., Cardou, A., Fiset, M. and Goudreau, S., 1994. Fretting fatigue in electrical transmission lines. *Wear*; 173:179–88.
- Zhou, Z.R., Cardou, A., Goudreau, S. and Fiset M., 1996. Fundamental investigations of electrical conductor fretting fatigue. *Tribol Int*; 29(3):221–32.
- Zhou, Z.R., Fayeulle, S. and Vincent, L., 1992. Cracking behaviour of various aluminium alloys during fretting wear. *Wear*;155:317–20.
- Zhou, Z.R., Gu, S.R. and Vicent L., 1997. An investigation of the fretting wear of two aluminium alloys. *Tribol Int*; 30:1–7.

8. RESPONSIBILITY NOTICE

The authors, Thamise Sampaio Vasconcelos Vilela, Aida Alves Fadel, Jorge Luiz de Almeida Ferreira e José Alexander Araújo, are the only responsible for the printed material included in this paper.